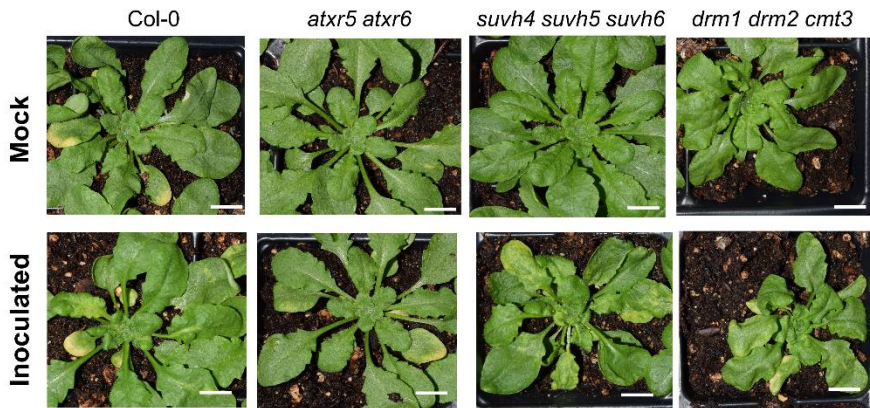


Supplementary Information

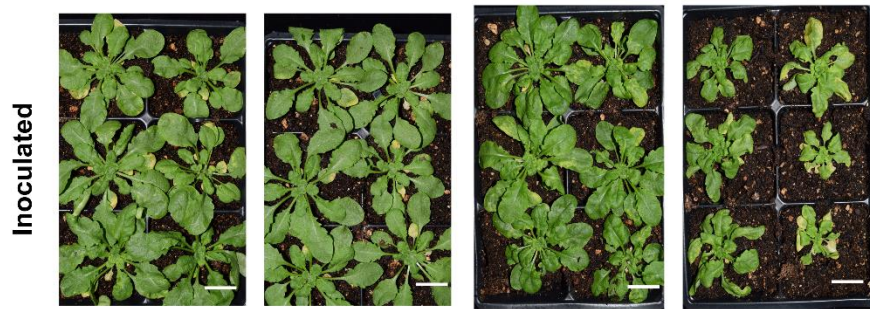
Title: H3.1K27me1 loss confers Arabidopsis resistance to Geminivirus by sequestering DNA repair proteins onto host genome

Zhen Wang, Claudia M. Castillo Gonzalez, Changjiang Zhao, Chun-Yip Tong, Changhao Li, Songxiao Zhong, Zhiyang Liu, Kaili Xie, Jiaying Zhu, Zhongshou Wu, Xu Peng, Yannick Jacob, Scott D. Michaels, Steven E. Jacobsen, Xiuren Zhang*

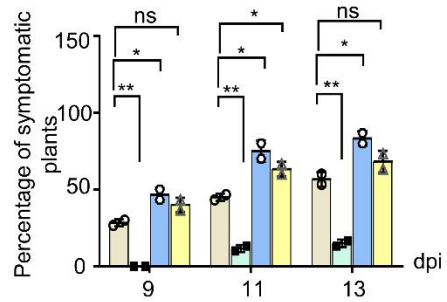
a



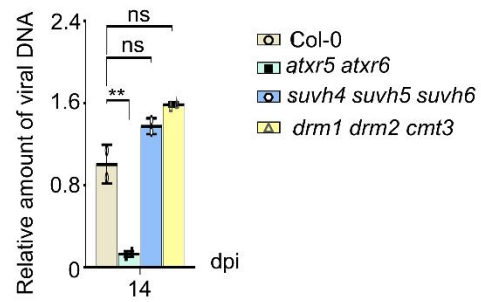
b



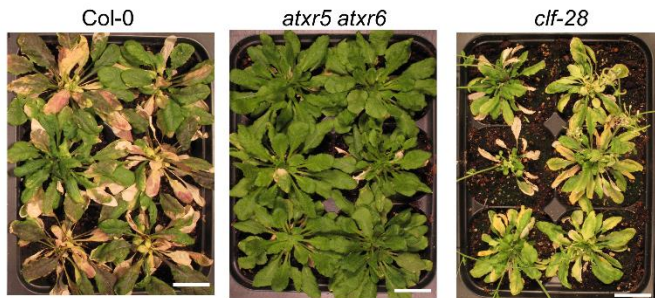
c



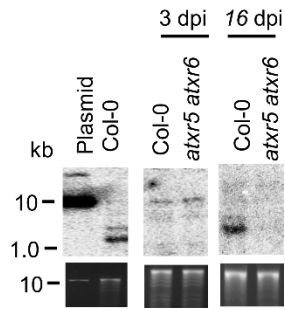
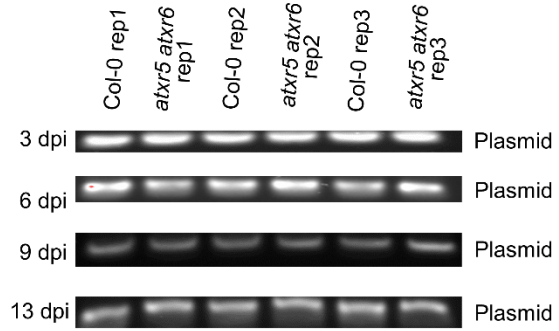
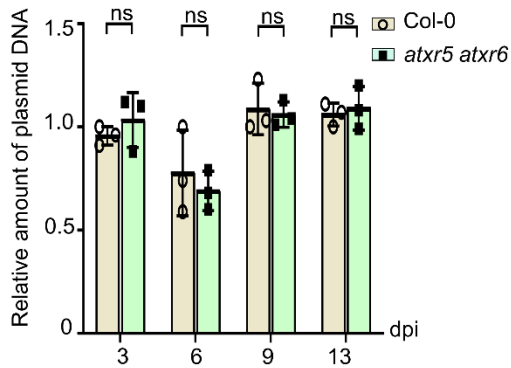
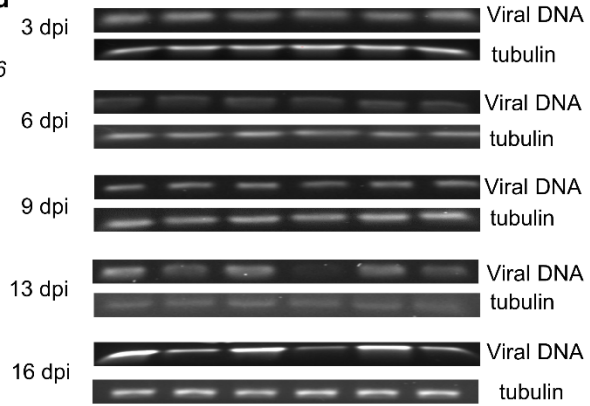
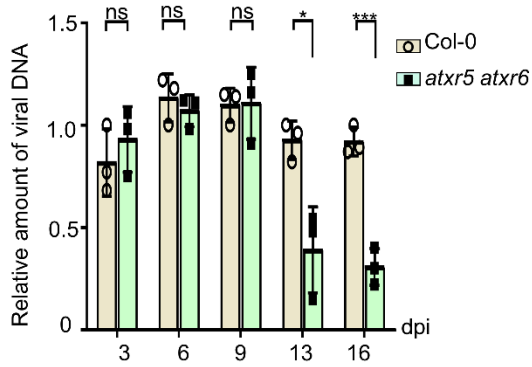
d



e

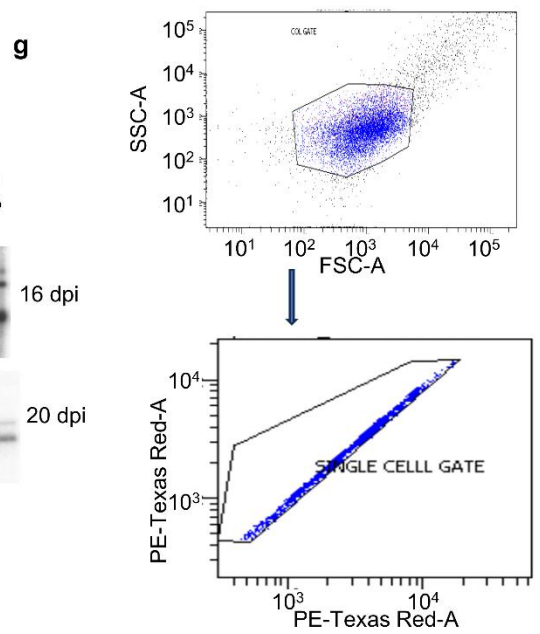
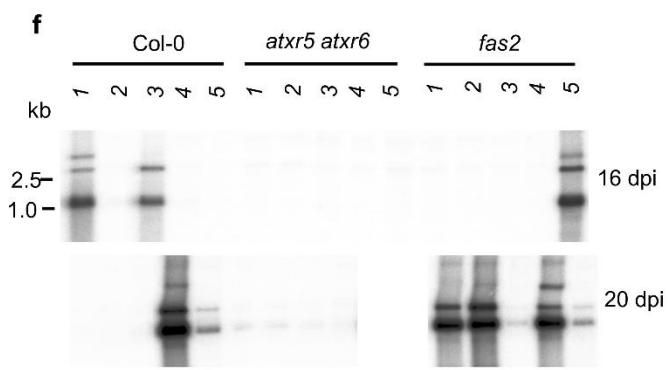
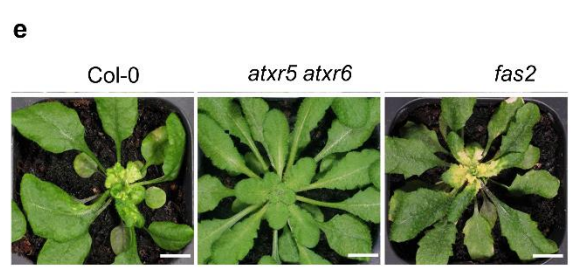
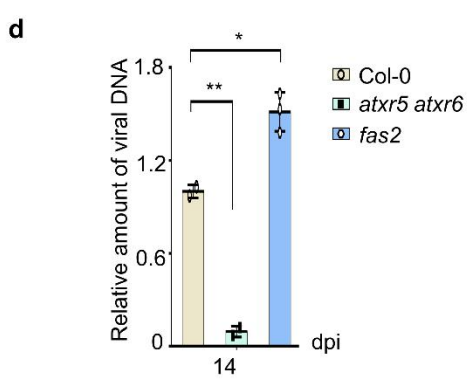
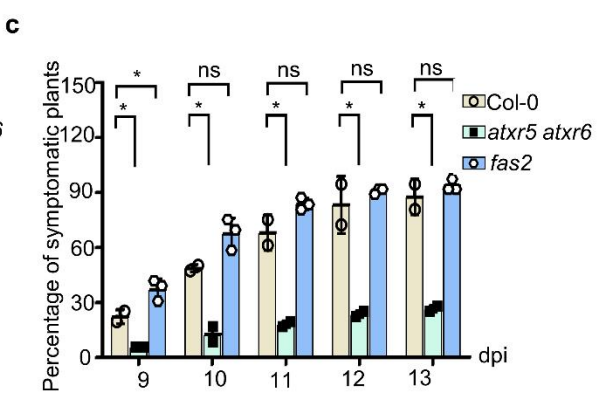
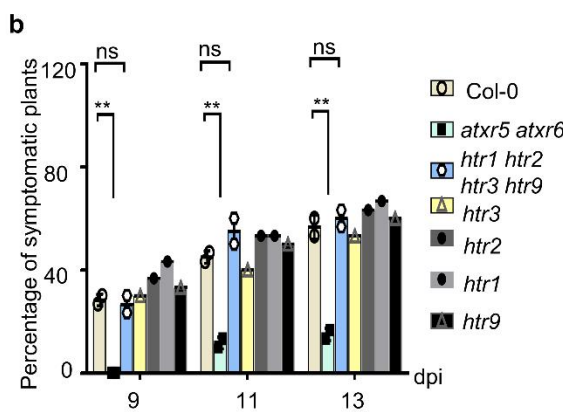
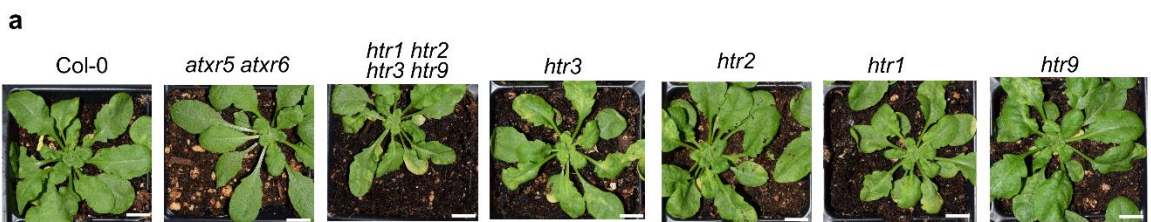


Supplementary Fig. 1. Loss of function mutants of *ATXR5* and *ATXR6*, different from other epigenetic mutants, display viral resistance phenotype. **a, b**, Representative pictures of the virus-inoculated plants in indicated backgrounds. Photographs were taken at 14 dpi. Scale bars, 1 cm (a). Scale bars, 2 cm (b). **c**, Percentages of symptomatic plants of virus-inoculated plants in indicated backgrounds at 9, 11, and 13 dpi. Each dot represents one biological replicate. The experiments were performed with 30 plants/replicate. Data are presented as mean \pm SD (n = 2 biological replicates). **d**, q-PCR assays show the amount of viral DNA in CaLCuV-inoculated plants indicated at 14 dpi. Data are presented as mean \pm SD (n = 2 biological replicates). Normalization of viral DNA was conducted as **Fig. 2g**. **e**, Representative pictures of the virus-inoculated plants in indicated backgrounds. Photographs were taken at 21 dpi. Scale bars, 2 cm. Statistics in **Supplementary Fig. 1c**, and **1d** was performed with unpaired two-tailed student t-test, *, **, *** and ****, $P < 0.05$, 0.01, 0.001, and 0.0001, respectively. Source data are provided in the Source Data File.

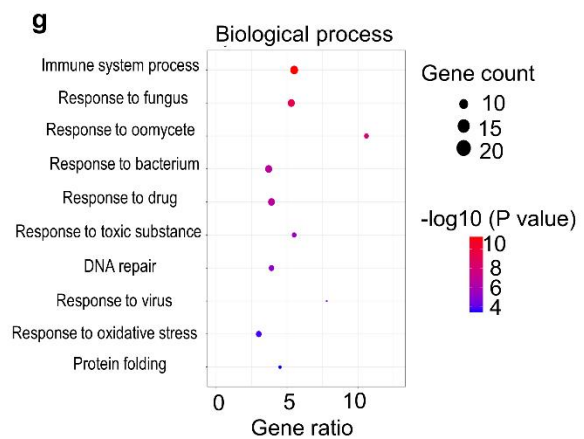
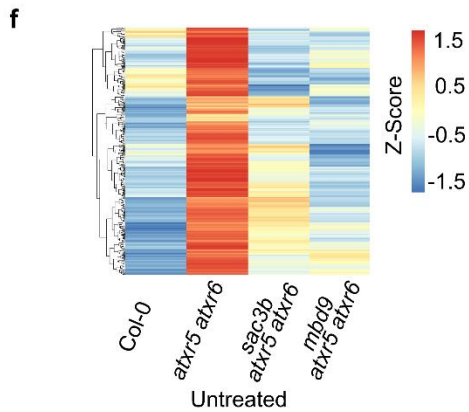
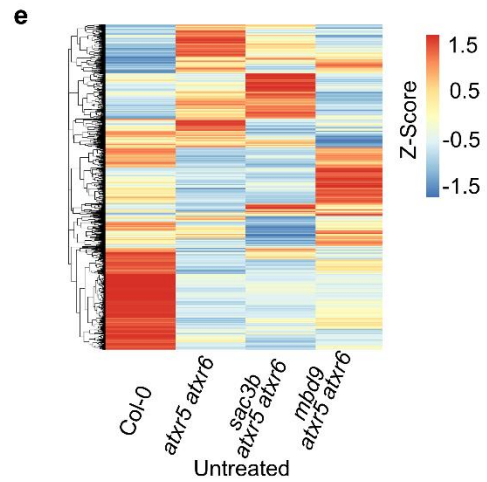
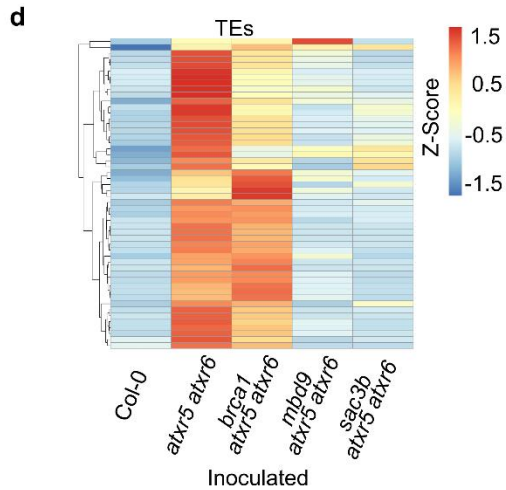
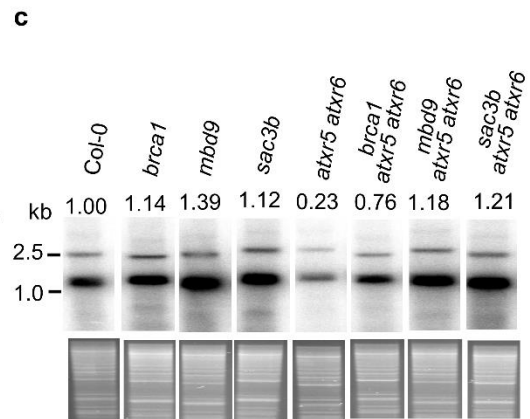
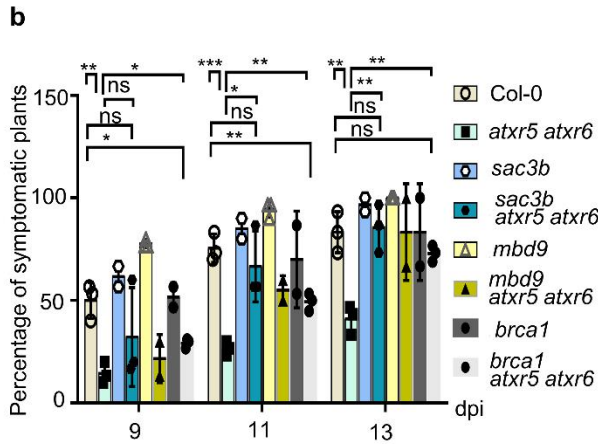
a**b****c****d****e**

Supplementary Fig. 2. Transfection efficiency is comparable between Col-0 and *atxr5*

atxr6. **a**, Southern blot assays showed the amount of delivered virus-contained plasmids (exemplified by 20 ng plasmid containing DNA A) and replicated viral DNA A (exemplified by 2 μ g total DNA from virus-inoculated Col-0 in Fig. 1g) in CaLCuV-inoculated Col-0 and *atxr5 atxr6* at 3 and 16 dpi. EcoRI digested input DNA served as a loading control (Bottom panel). The experiments were repeated twice with similar results. **b**, Semi-quantitative PCR analysis to test the delivered plasmid levels in Col-0 and *atxr5 atxr6* at 3, 6, 9, and 13 dpi. *Tubulin* served as a control. The experiments were repeated two times with similar results. **c**, Quantitative-PCR assays to test virus plasmid level. The plasmid DNA detected by q-PCR was normalized against the *tubulin*, and then to Col-0 where the internally normalized viral titer of replicate 1 was arbitrarily assigned as a value of 1 at each time point. Each dot in the bar plot represents one replicate, experiments were performed with 6 plants/replicate. Data are presented as mean \pm SD (n = 3 biological replicates). **d**, Semi-quantitative PCR analysis to test virus DNA levels in Col-0 and *atxr5 atxr6* at 3, 6, 9, and 13 dpi. *Tubulin* served as a control. The experiments were repeated twice with similar results. **e**, Quantitative-PCR assays to test virus DNA levels. Samples for **b**, **c**, **d**, and **e** come from the same set materials. Each dot in the bar plot represents one replicate, experiments were performed with 6 plants/replicate. Data are presented as mean \pm SD (n = 3 biological replicates). Normalization was conducted according to **Supplementary Fig. 2c**. Statistics in **Supplementary Fig. 2c**, and **2e** were performed with unpaired two-tailed student t-test, *, **, *** and ****, $P < 0.05$, 0.01, 0.001, and 0.0001, respectively. Source data are provided in the Source Data File.

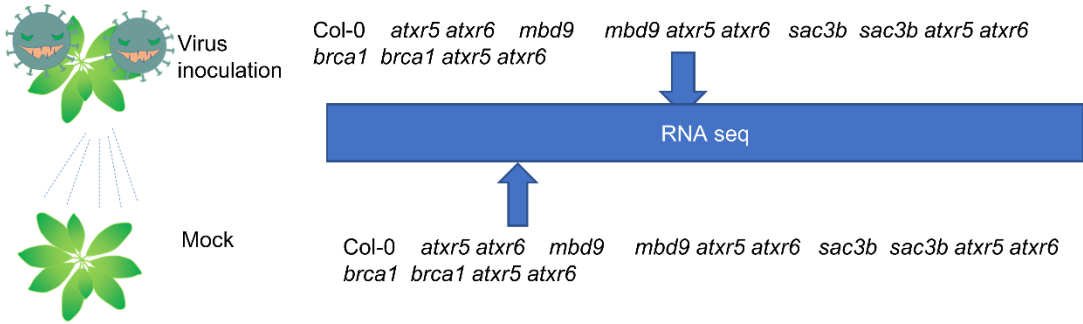


Supplementary Fig. 3. H3.1 single and quadruple mutants and *fas-2*, unlike *atx5 atx6*, are hyper-susceptible to viral infection. **a**, Representative pictures of the virus-inoculated Col-0, *atx5 atx6*, *htr1*, *htr2*, *htr3*, *htr9*, and *htr1 htr2 htr3 htr9* mutants. Photographs were taken at 14 dpi. Scale bars, 1 cm. **b**, Percentages of symptomatic plants of CaLCuV-inoculated Col-0, *atx5 atx6*, *htr1*, *htr2*, *htr3*, *htr9* and *htr1 htr2 htr3 htr9* mutants at 9, 11, and 13 dpi. Each dot in the bar plot represents one replicate, experiments were performed with 30 plants/replicate. Data are presented as mean \pm SD ($n = 2$ biological replicates for Col-0, *atx5 atx6*, and *htr1 htr2 htr3 htr9*; $n = 1$ biological replicate for *htr3*, *htr2*, *htr1*, *htr9*). **c**, Percentages of symptomatic plants of CaLCuV-inoculated Col-0, *atx5 atx6* and *fas2* mutants at 9, 10, 11, 12, and 13 dpi. Each dot in the bar plot represents one replicate, experiments were performed with 36 plants/replicate. Data are presented as mean \pm SD ($n = 2$ biological replicates for Col-0 and *atx5 atx6*; $n = 3$ biological replicate for *fas2*). **d**, Quantitative-PCR assays showed the amount of viral DNA in CaLCuV-inoculated Col-0, and *fas2* at 14 dpi. Each dot in the bar plot represents one replicate, experiments were performed with 36 plants/replicate. Data are presented as mean \pm SD ($n = 2$ biological replicates for Col-0 and *atx5 atx6*; $n = 3$ biological replicate for *fas2*). The relative amount of viral DNA was normalized as described in **Fig. 2g**. **e**, Representative pictures of the virus-inoculated Col-0, *atx5 atx6*, and *fas2* at 21 dpi. Each dot in the bar plot represents one replicate, experiments were performed with three biological replicates (36 plants/replicate). Scale bars, 1cm. **f**, Southern blot analysis showed that the amount of viral DNA in CaLCuV-inoculated individual plants of Col-0, *atx5 atx6*, and *fas2* mutants at 16 and 20 dpi. The experiments were repeated twice with similar results. **g**. The schematic diagram of experimental designs to collect sufficient intact protoplast ($n=10000$, Texas Red >400) to perform flow cytometry analysis. Statistics in **Supplementary Fig. 3b**, **3c**, and **3d** were performed with unpaired two-tailed student t-test, *, **, *** and ****, $P < 0.05$, 0.01, 0.001, and 0.0001, respectively. The comparison between Col-0 and *fas2* in **Supplementary Fig. 3c**, and **3d** was performed with unpaired two-tailed student t-test with Welch's correction. Source data are provided in the Source Data File.

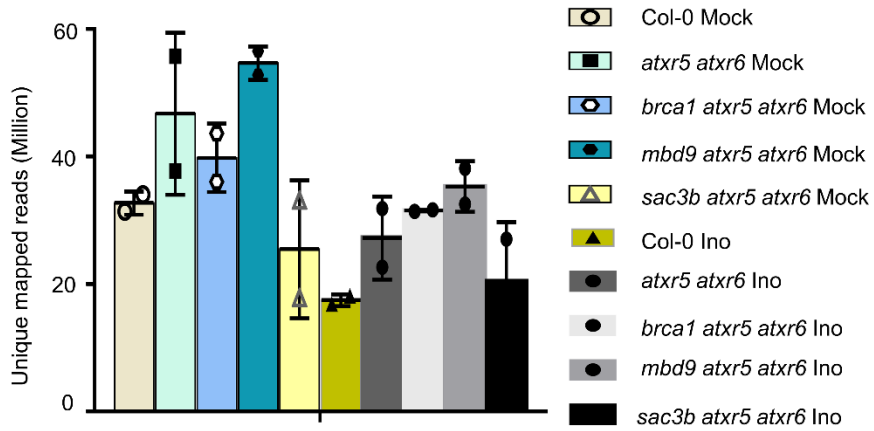


Supplementary Fig. 4. The molecular phenotype of TE reactivation is uncoupled with the viral resistance phenotype in *atx5 atx6*. **a**, The loss of *MBD9*, *SAC3B*, or *BRCA1* could all increase viral susceptibility of *atx5 atx6*. Photographs of CaLCuV-inoculated plants were taken at 14 dpi. Scale bars, 1 cm. **b**, Percentages of symptomatic plants in different backgrounds induced by CaLCuV-inoculation at 9, 11, and 13 dpi. Each dot in the bar plot represents one replicate, experiments were performed with 30 plants/replicate. Data are presented as mean \pm SD (n = 3 biological replicates for Col-0, *atx5 atx6*, *sac3b atx5 atx6*, *brca1 atx5 atx6*, and *mbd9*; n = 2 biological replicates for *brca1*, *sac3b*, and *mbd9 atx5 atx6*). **c**, Southern blot assays showed that the accumulation of viral DNA in CaLCuV-inoculated plants with different genotypes at 14 dpi. The experiments were repeated two times with similar results. EcoRI-digested input DNA serves as a loading control (Bottom panel). Scale bars, 2 cm. **d**, Heat map showed the change of transcript levels for TEs in virus-inoculated Col-0, *atx5 atx6*, *mbd9 atx5 atx6*, *brca1 atx5 atx6*, and *sac3b atx5 atx6*. The quantification was conducted by DESeq2. **e**, Heat map showed the overall change of transcript level for 1625 DEGs in *atx5 atx6*, *mbd9 atx5 atx6*, and *sac3b atx5 atx6*. RNA-seq data were mined from GSE77735. The quantification was done with DESeq2. **f**, Heat map showed the transcriptional level change for 240 genes selected from 1625 DEGs in indicated backgrounds. **g**, Bubble plots showed the enrichment of 240 DEGs in different GO biological. Statistics in **Supplementary Fig. 4b** were performed with unpaired two-tailed student t-test, *, **, *** and ****, $P < 0.05$, 0.01, 0.001, and 0.0001, respectively. Source data are provided in the Source Data File.

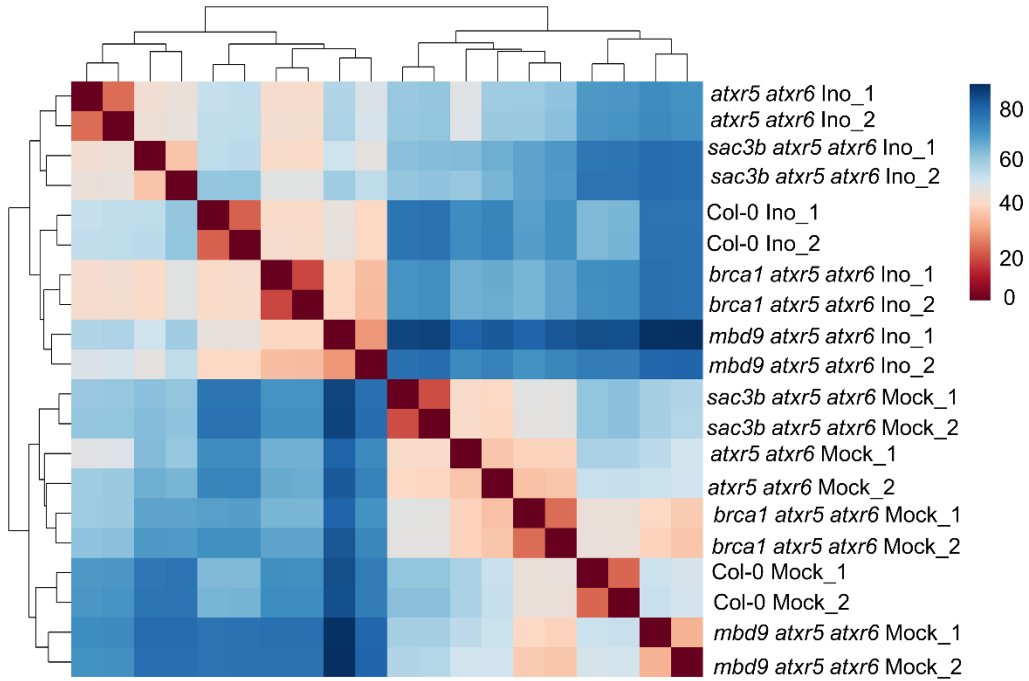
a



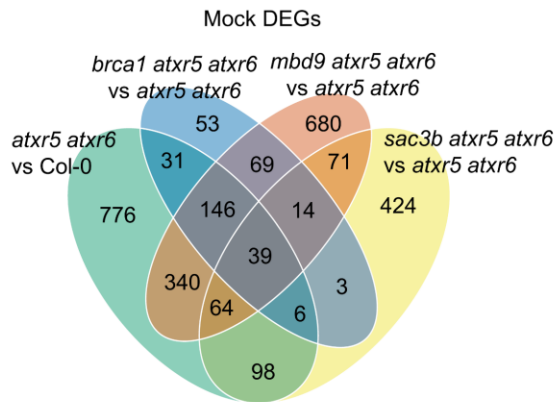
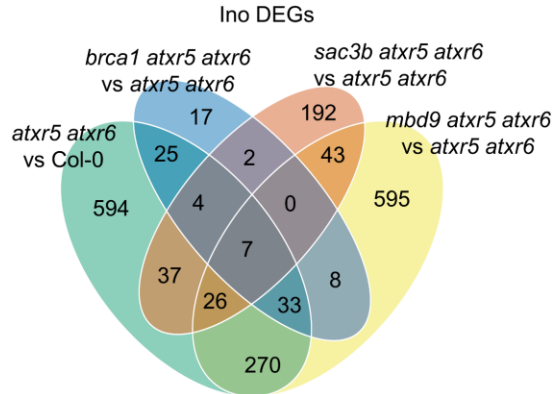
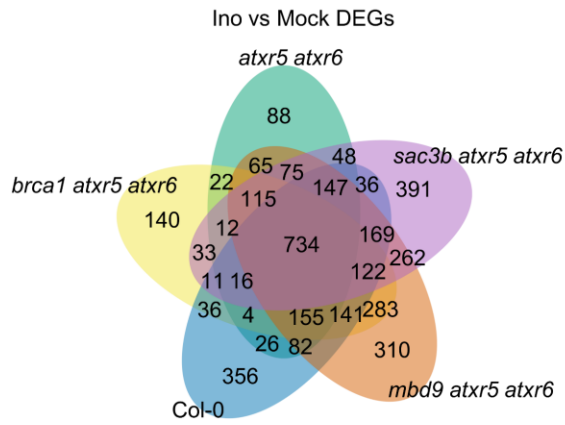
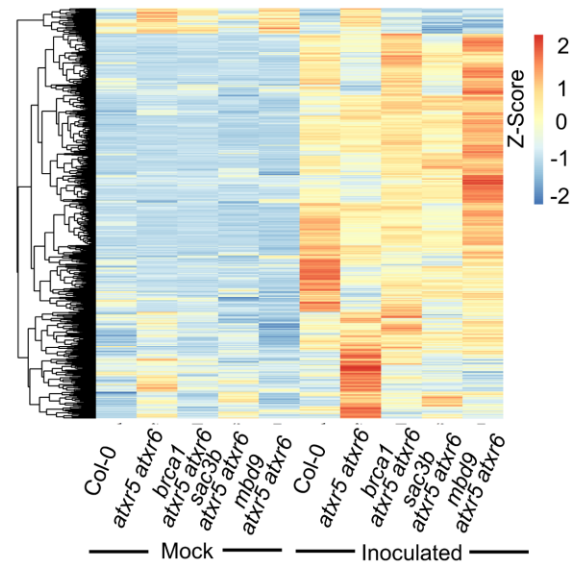
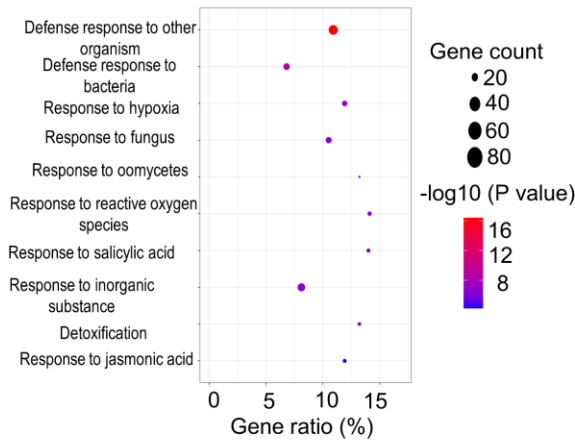
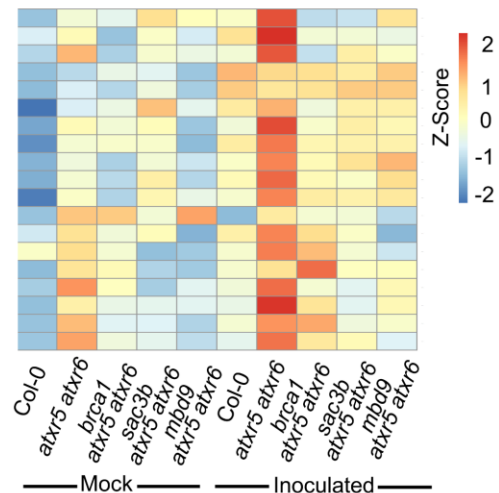
b



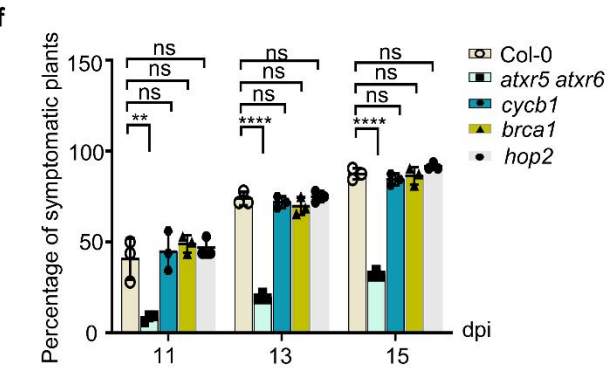
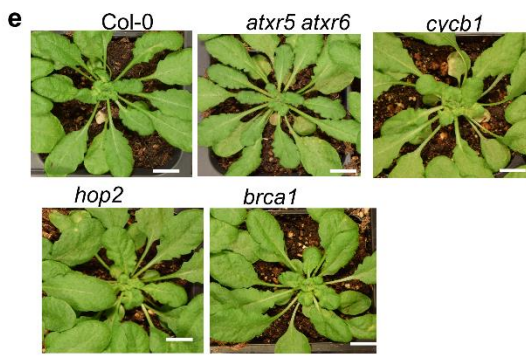
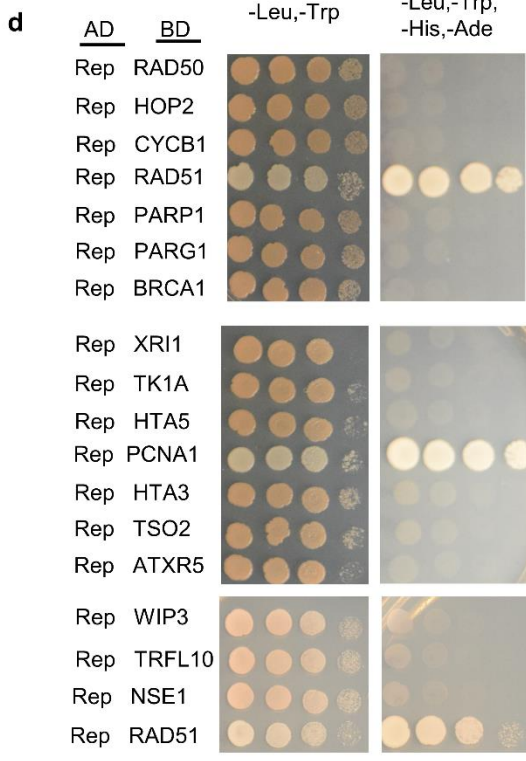
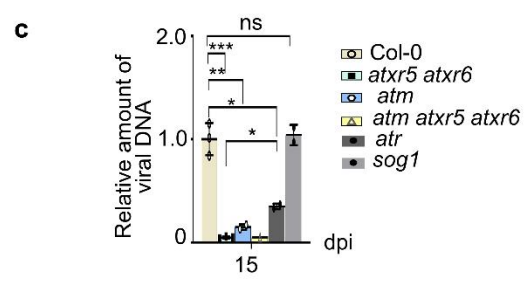
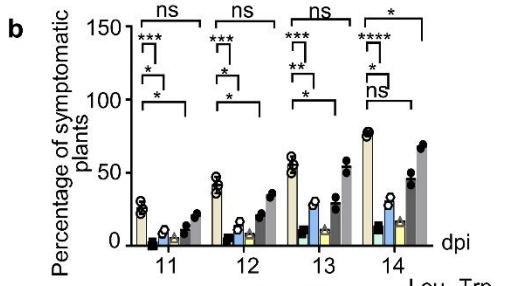
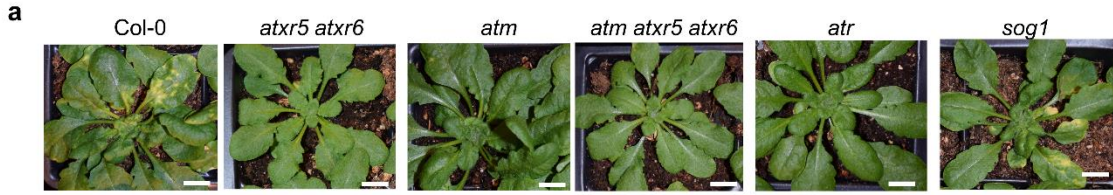
c



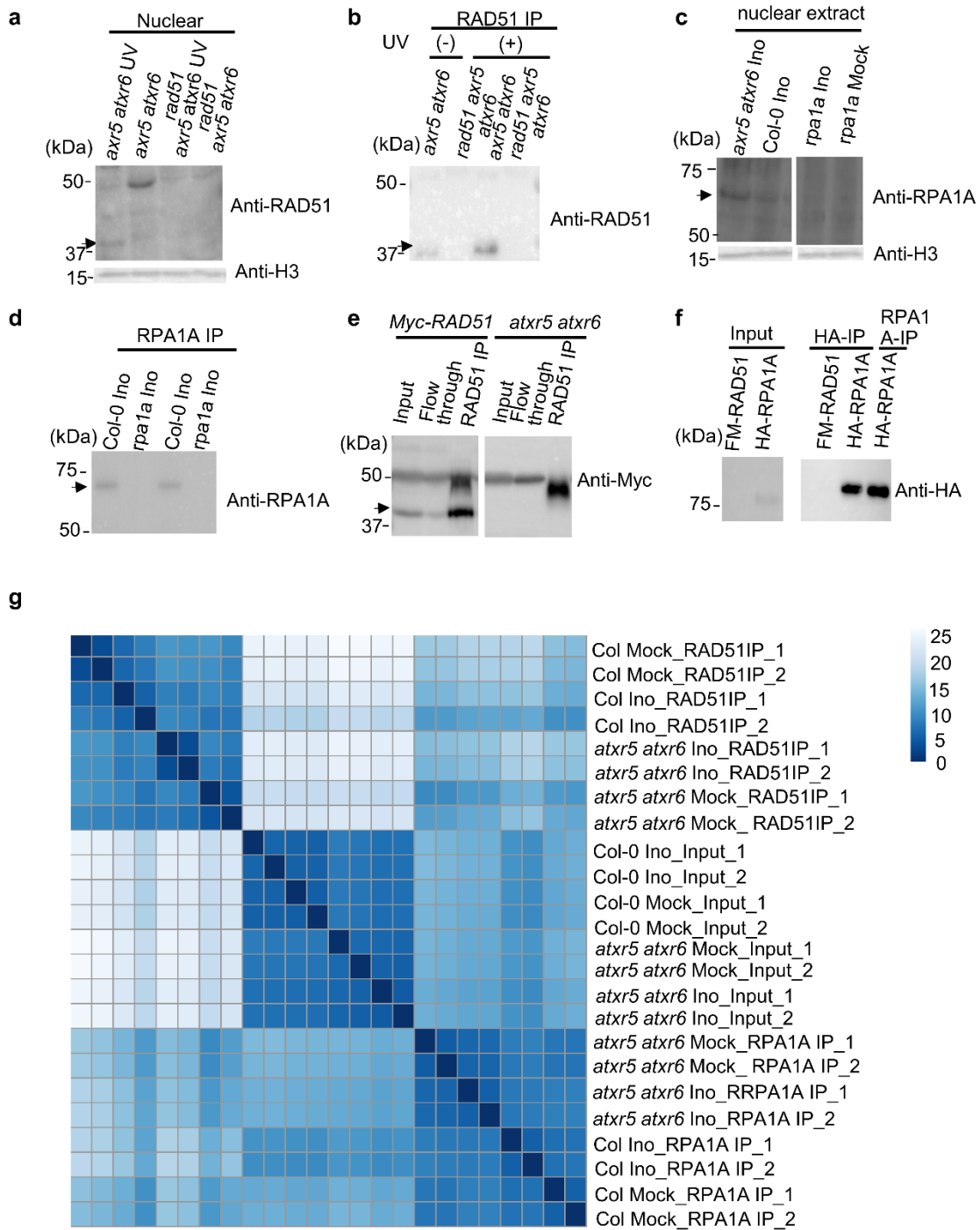
Supplementary Fig. 5. Highly reproducible datasets show high quality of RNA-seq. **a**, The schematic diagram of experimental designs for viral inoculation and sample collection timing for RNA-seq. Each tray was separated into 6 parts and each part contained 6 individual plants. Figure is drawn with Microsoft Power Point. **b**, Summary of unique mapped reads used for following RNA-seq analysis. Ino represents viral-inoculated plants. **c**, Heatmap of sample clustering shows the high reproducibility within treatments for tested lines in RNA-seq.

a**b****c****d****e****f**

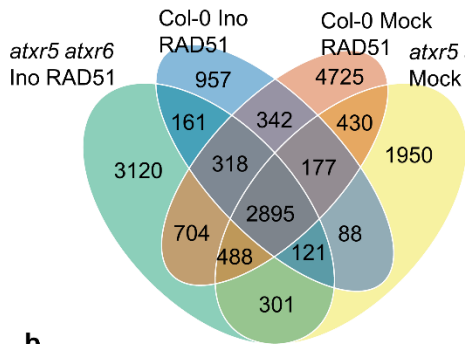
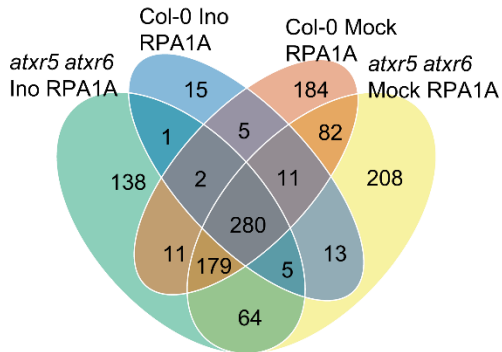
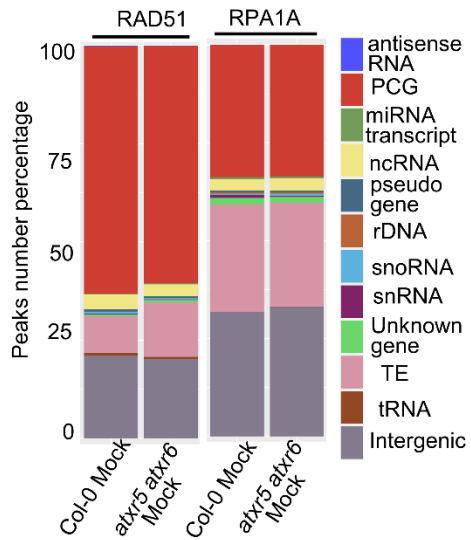
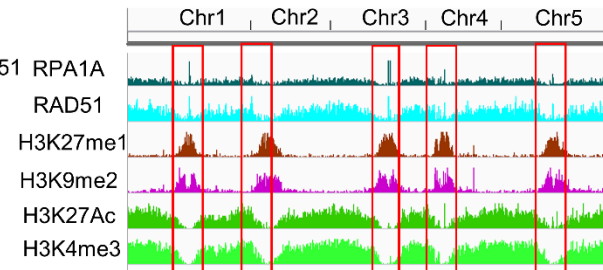
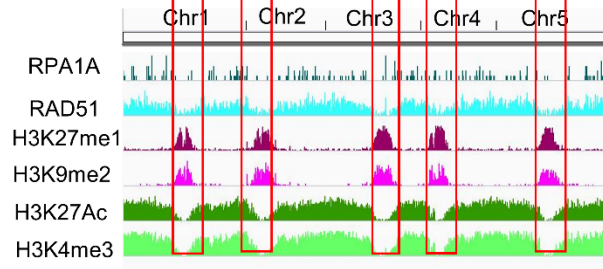
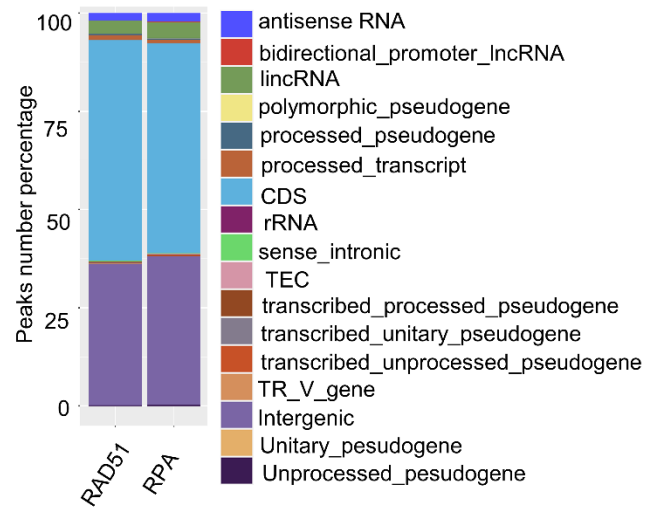
Supplementary Fig. 6. TWAS analysis identified the genes that are highly correlated with viral resistance of *atxr5 atxr6*. **a**, Venn diagram shows the overlap between DEGs from mock-treated samples. **b**, Venn diagram shows the overlap between DEGs from virus-inoculated samples. **c**, Venn diagram shows the DEGs between mock-treated and virus-inoculated samples. **d**, Heat map shows the changes of transcript levels for approximately 1100 selected genes from approximately 4800 differentially expressed genes from **a**, **b**, and **c** in mock-treated and virus-inoculated Col-0, *atxr5 atxr6*, *brca1 atxr5 atxr6*, *sac3b atxr5 atxr6*, and *mbd9 atxr5 atxr6* plants. **e**, Bubble plots show enrichment of DEGs from **d** in different GO biological processes. **f**, Heat map shows the changes of transcript levels for 19 genes related to DNA damage response (DDR) in mock-treated and virus-inoculated Col-0, *atxr5 atxr6*, *brca1 atxr5 atxr6*, *sac3b atxr5 atxr6*, and *mbd9 atxr5 atxr6* plants.



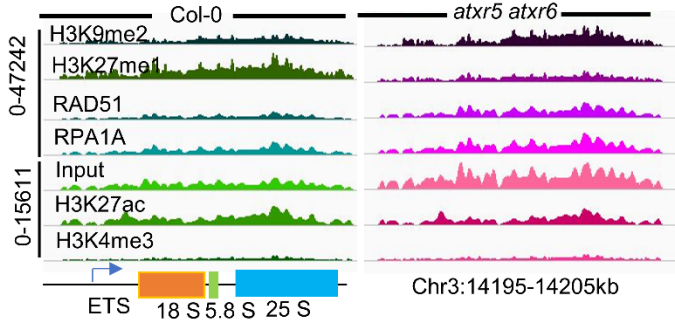
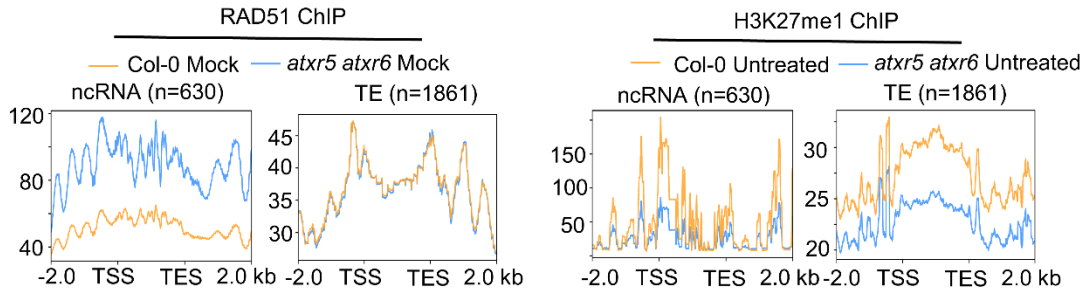
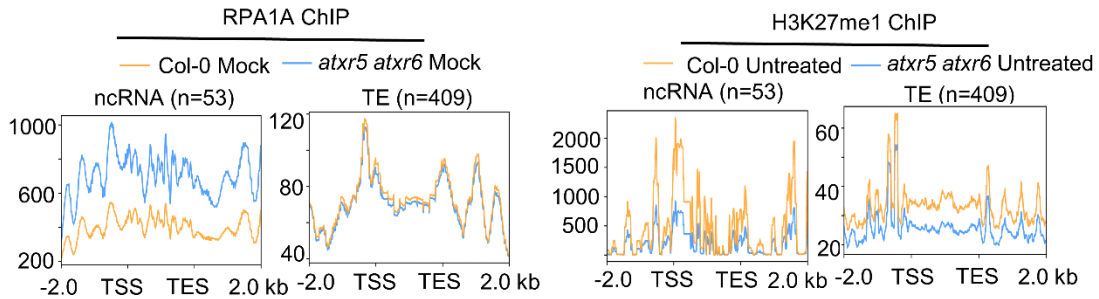
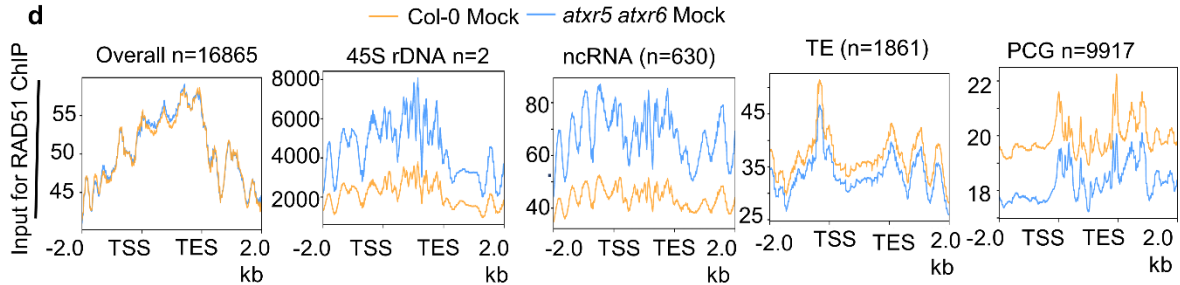
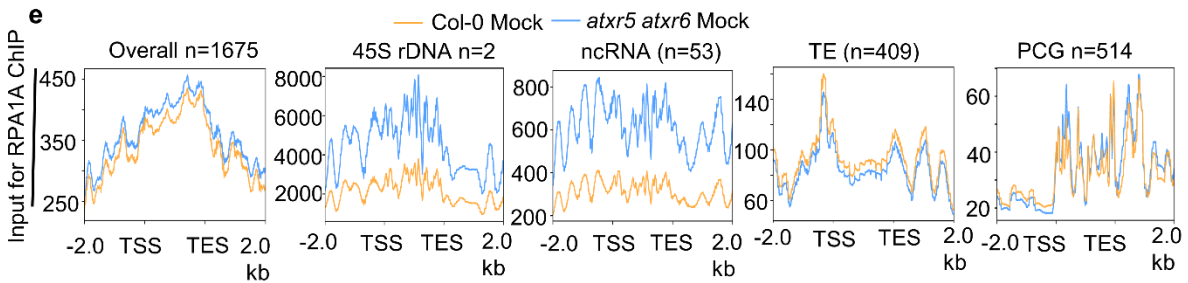
Supplementary Fig. 7. Y2H screening of HRR proteins identify a few Rep-interacting proteins. **a**, Representative phenotypes of CaLCuV-inoculated Col-0, *atx5 atx6*, *atm*, *atx5 atx6 atm*, *atr*, and *sog1* plants. Photographs were taken at 15 dpi. Scale bars, 1 cm. **b**, Percentages of symptomatic plants induced by CaLCuV-inoculation in indicated backgrounds at 11, 12, 13, and 14 dpi. Each dot in the bar plot represents one replicate, experiments were performed with 32 plants/replicate. Data are presented as mean \pm SD (n = 3 biological replicates for Col-0 and *atx5 atx6*; n = 2 biological replicates for *atm*, *atr*, and *sog1*; n = 1 biological replicate for *atx5 atx6 atm*). **c**, q-PCR shows the amount of viral DNA A in CaLCuV-inoculated plants in indicated backgrounds at 15 dpi. Each dot in the bar plot represents one replicate, experiments were performed with 32 plants/replicate. Data are presented as mean \pm SD (n = 3 biological replicates for Col-0 and *atx5 atx6*; n = 2 biological replicates for *atm*, *atr* and *sog1*; n = 1 biological replicate for *atx5 atx6 atm*). The relative amount of viral DNA A was normalized as described in **Fig. 2g**. **d**, Y2H screening pinpointed the *bona fide* targets of Rep. **e**, Representative pictures of the virus-inoculated Col-0, *atx5 atx6*, *cycb1*, *hop2*, and *brca1* plants. Photographs were taken at 16 dpi. **f**, Percentages of symptomatic plants of CaLCuV-inoculated Col-0, *atx5 atx6*, *cycb1*, *hop2*, and *brca1* mutants at 11, 13, and 15 dpi. Each dot in the bar plot represents one replicate, experiments were performed with 32 plants/replicate. Data are presented as mean \pm SD (n = 3 biological replicates). Statistics in **Supplementary Fig. 7b**, **7c**, and **7f** were performed with unpaired two-tailed student t-test, *, **, *** and ****, $P < 0.05$, 0.01, 0.001, and 0.0001, respectively. The comparisons between Col-0 and *atm*, *sog1*, or *atr* in **Supplementary Fig. 7b**, **7c**, were performed with unpaired two-tailed student t-test with Welch's correction. Source data are provided in the Source Data File.



Supplementary Fig. 8. Quality analysis of ChIP-seq for RAD51 and RPA1A. **a, c,** Western blot analyses with isolated nuclei from plants with indicated genotypes and treatments using anti-RAD51 (a) and anti-RPA1A (c) antibodies. The experiments were repeated twice with similar results. **b, d,** Western blot analysis with immunoprecipitated RAD51 (b) and RPA1A (d) validated the specificity of anti-RAD51 and anti-RPA1A antibodies. The anti-RAD51 and anti-RPA1A antibodies were conjugated to protein A magnetic beads prior to immunoprecipitation. The experiments were repeated twice with similar results. **e,** Western blot analysis using an anti-Myc antibody validated the specificity of the anti-RAD51 antibody used for immunoprecipitation. The IP of Myc-RAD51 is performed with an anti-RAD51 antibody in *Arabidopsis*. The experiments were repeated twice with similar results. **f,** Western blot analysis using an anti-HA antibody validated the specificity of the anti-RPA1A antibody for immunoprecipitation. The IP of HA-RPA1A is performed with anti-RPA1A in *N. benthamiana*. IP with anti-HA served as a positive control for IP with anti-RPA1A. The experiments were repeated twice with similar results. **g,** Heatmap of sample clustering shows high reproducibility between treatments for tested lines. Source data are provided in the Source Data File.

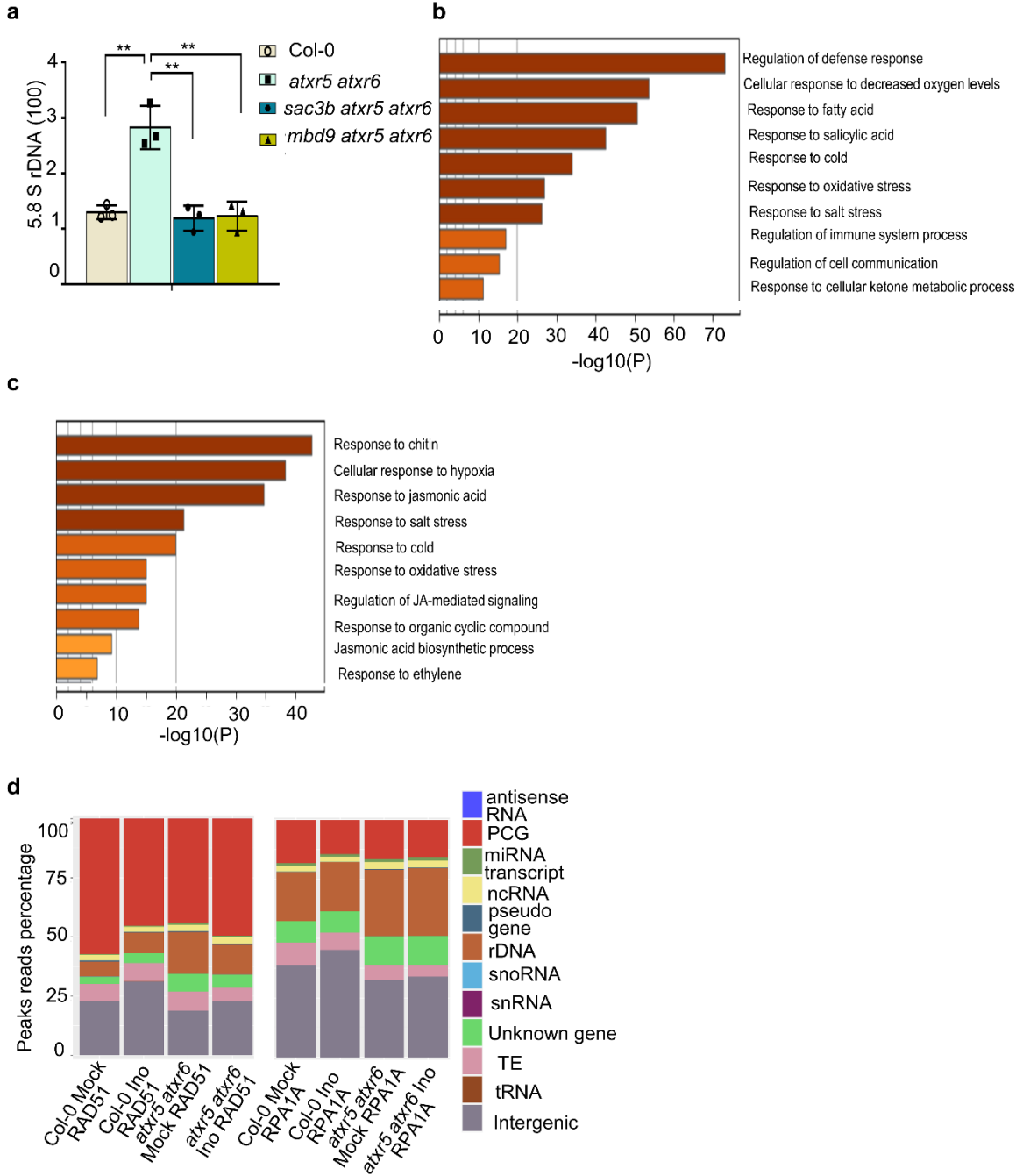
a**b****e****c****d****f**

Supplementary Fig. 9. Distributions of RAD51-bound peak over euchromatin and heterochromatin regions. **a, b** Venn diagram shows the overlap of RAD51 (a), and RPA1A (b)-bound peaks among different genotypes and treatments. **c**, Chart diagrams show peak distributions of RPA1A, RAD51, H3K27me1, H3K9me2, H3K4me3, and H3K27Ac over genome of Col-0. Be noted: total mapping reads which contained multiple mapping reads were used to perform peak calling analysis (see methods). H3K9me2 and H3K27me1 related data were mined from published data (GSE111814), H3K4me3 related data were mined from published data (GSE166897), H3K27Ac related data were mined from GSE146126. **d**, Chart diagrams show the peak distributions of RPA1A, RAD51, H3K27me1, H3K9me2, H3K4me3, and H3K27Ac over genome of Col-0. Be noted that the unique mapping reads which does not contain multiple mapping reads are used to perform peak calling analysis. **e**, Genomic feature classification of RAD51 and RPA enriched regions in Col-0 and *atx5 atx6*. The y axis represents the percentages of peak numbers belonging to various categories. Peak identification using total mapped reads. **f**, Genomic feature classification of RAD51 and RPA enriched regions over genome of *Mus musculus*. The y axis represents the percentages of peak numbers belonging to various categories. Peak identification using total mapped reads. RAD51 and RPA related data were mined from published data (GSE143582). Source data are provided in the Source Data File.

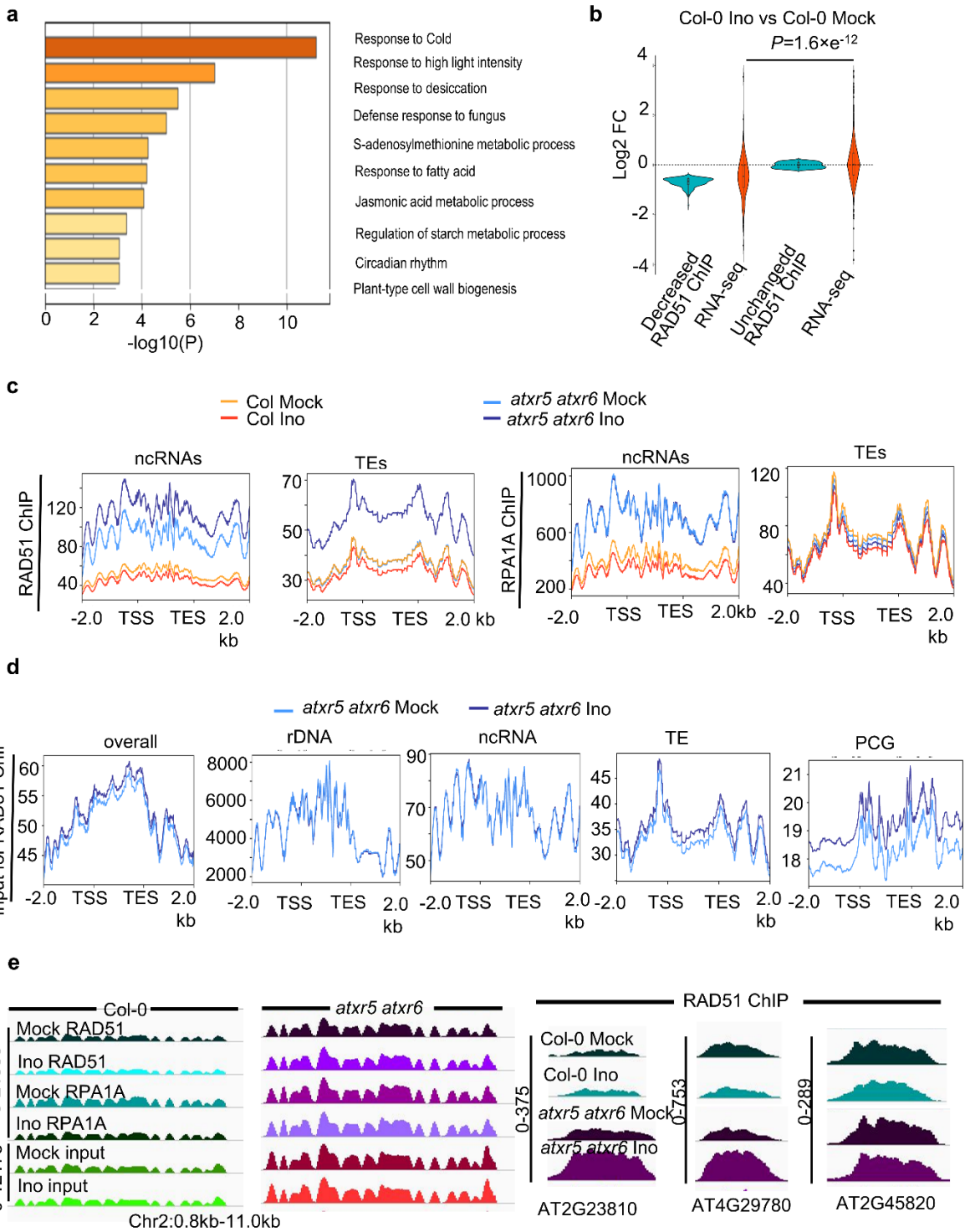
a**b****c****d****e**

Supplementary Fig. 10. ChIP signal of RAD51 and RPA1A in mock-treated Col-0 and *atx5*

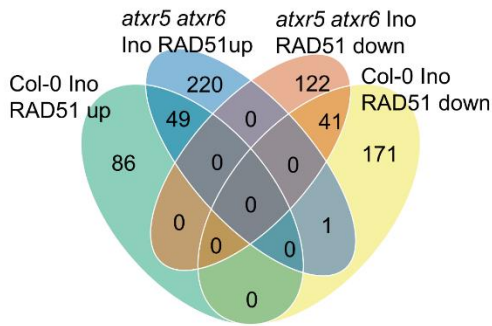
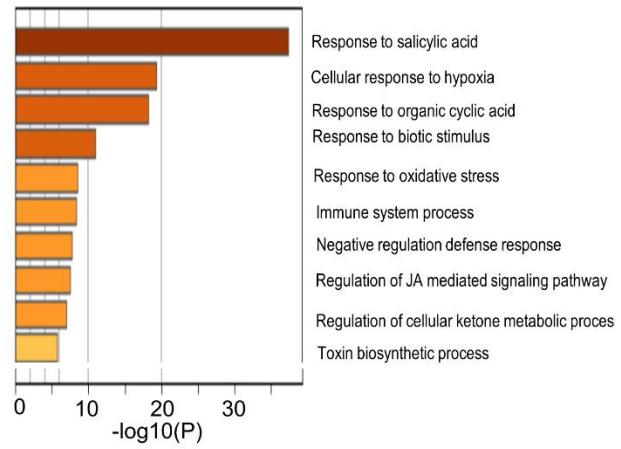
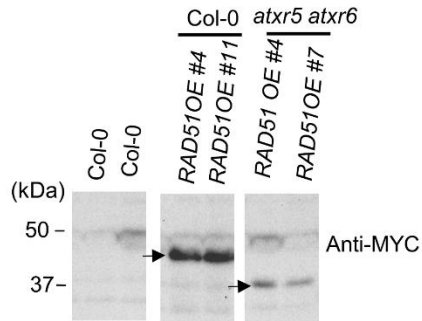
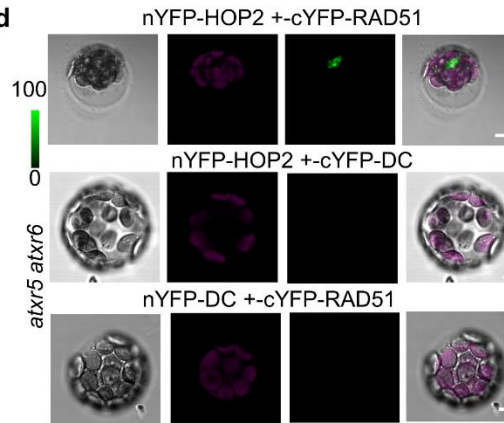
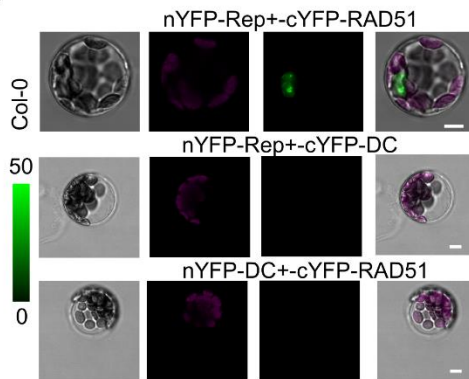
atx6. **a**, IGV files of normalized ChIP signals (RPKM) of H3K9me2, H3K27me1, RAD51 (normalized with the reads of mitochondrial DNA), RPA1A (normalized with the reads of mitochondrial DNA), H3K27ac and H3K4me3 on a *45S rDNA* locus on chr3. H3K9me2 and H3K27me1 related data were mined from published data (GSE111814), H3K4me3 related data were mined from GSE166897, H3K27Ac related data were mined from GSE146126. Scales for the distinct loci were shown in left as solid lines. **b**, Distribution of normalized RAD51 ChIP-signal (normalized with the reads of mitochondrial DNA), and H3K27me1(RPKM) from Col-0 and *atx5 atx6* over RAD51-enriched different categories. H3K27me1 related data were mined from GSE111814. **c**, Distribution of normalized RPA1A ChIP-signal (normalized with the reads of mitochondrial DNA), and H3K27me1 (RPKM) from Col-0 and *atx5 atx6* over RPA1A enriched different categories. H3K27me1 related data were mined from GSE111814. **d**, Distribution of normalized input reads (RPKM) from Col-0 and *atx5 atx6* plants on different categories of RAD51 enriched regions. **e**, Distribution of normalized input reads from Col-0 and *atx5 atx6* plants on different categories of RPA1A enriched regions.



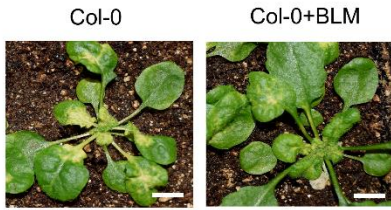
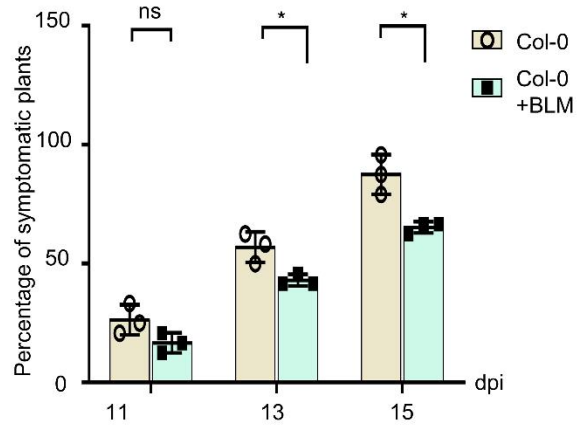
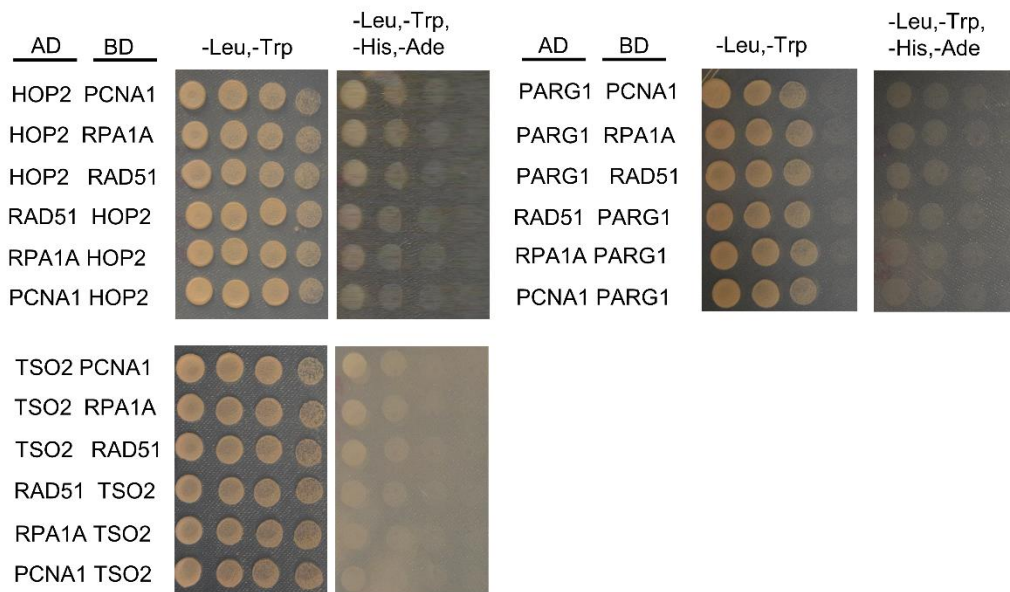
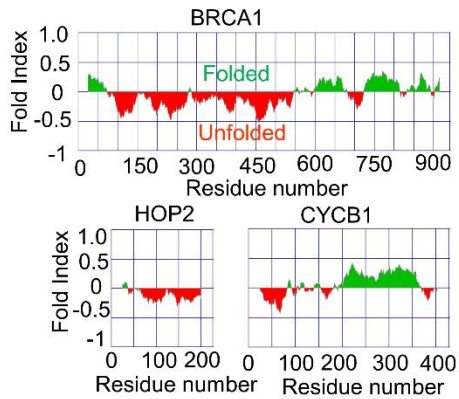
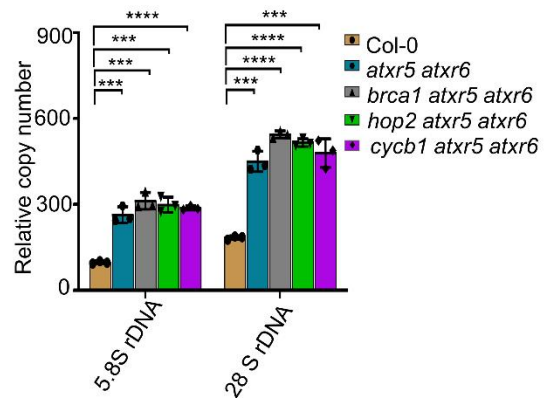
Supplementary Fig. 11. Gene Ontology (GO) analysis of RAD51 and RPA1A enriched PCGs. **a**, q-PCR shows the amount of rDNA in Col-0, *atxr5 atxr6*, *mbd9 atxr5 atxr6*, and *sac3b atxr5 atxr6*. The relative amount of rDNA was normalized against *UBQ10* (Unpaired two tailed student t-test, *, **, *** and ****, $P < 0.05$, 0.01, 0.001, and 0.0001, respectively). Each dot in the bar plot represents one replicate, the experiments were performed with 36 plants/replicate. Data are presented as mean \pm SD ($n = 3$ biological replicates). **b**, GO analysis shows the enrichment of RAD51 enriched top 3000 genes filtered by P -value in different biological processes. **c**, GO analysis show the enrichment of RPA1A-enriched genes in different biological processes. **d**, Peak reads distributions of RAD51 and RPA1A ChIP-seq in various locus categories in Col-0 and *atxr5 atxr6*. The y axis represents the percentage of reads mapped to loci belonging to various categories. GO analysis in the **Supplementary Fig. 11 b, c** was done via Metascape[<https://metascape.org>]. Source data are provided in the Source Data File.



Supplementary Fig. 12. The change of RAD51 and RPA1A signal induced by viral infection in Col-0 and *atxr5 atxr6*. **a**, GO analysis of PCGs show the decreased RAD51 signal over the indicated pathways in Col-0 upon viral inoculation. Go analysis was done via Metascape[<https://metascape.org>]. **b**, Violin plot shows the transcript changes from the loci with reduced and unchanged RAD51 ChIP signal in viral-inoculated Col-0 vs Mock-treated Col-0. Horizontal lines in the bar plots display the 75th percentile, median, and 25th percentile, respectively. Whiskers represents the minimum and maximum values. *P* value is calculated by unpaired two-tailed Welch's approximate *t*-test. **c**, Distribution of normalized RAD51 and RPA1A ChIP-signal (normalized with the reads of mitochondrial DNA) from mock-treated and virus-inoculated Col-0 and *atxr5 atxr6* over RAD51 or RPA1A enriched different categories. **d**, Distribution of normalized input reads (RPKM) from mock-treated and virus-inoculated *atxr5 atxr6* on different categories of RAD51-enriched regions. **e**, IGV files show changes of RAD51 and RPA1A signal of an rDNA loci and indicated PCGs in mock-treated and virus-inoculated Col and *atxr5 atxr6* (normalized by RPKM). Scales for the distinct loci were shown in left as solid lines.

a**b****c****d****e**

Supplementary Fig. 13. Viral infection enhances the RAD51 signal over PCGs related to defense response. **a**, Venn graph shows change of RAD51 signal from enriched peaks over host genome in Col-0 and *atx5 atx6* upon virus inoculation. **b**, GO analysis of PCGs show the enhanced RAD51 signal in *atx5 atx6* upon viral infection. GO analysis was done via Metascape tool⁷⁶. **c**, Western blots analysis of RAD51 transgenic lines in Col-0 and *atx5 atx6* backgrounds (head arrows indicate the Flag-4Myc-RAD51 in Col-0 or 6Myc-RAD51 in *atx5 atx6*). The experiments were repeated twice with similar results. **d**, Confocal images showed the interaction between HOP2 and RAD51 in protoplasts from the indicated backgrounds. nYFP-DC and cYFP-DC served as negative controls. Scale bars, 5 μ m. **e**, Confocal images showed the interaction between Rep and RAD51 in protoplasts from the indicated backgrounds. nYFP-DC and cYFP-DC served as negative controls. Scale bars, 5 μ m. Source data are provided in the Source Data File.

a**b****c****d****e**

Supplementary Fig. 14. Deletions of HOP2, BRCA1, and CYCB1 do not affect the viral DNA replication. **a**, Representative phenotypes of CaLCuV-inoculated plants in the indicated background and treatment. Photographs were taken at 15 dpi. Scale bars, 2 cm. **b**, Percentages of symptomatic plants induced by CaLCuV-inoculation in the indicated background and treatment at 11, 13, and 15 dpi. Each dot in the bar plot represents one replicate, experiments were performed with 24 plants/replicate. Data are presented as mean \pm SD ($n = 3$ biological replicates). **c**, Y2H assays to test the interaction between RAD51, RPA1A and selected candidate factors. **d**, Folding prediction of HOP2, BRCA1 and CYCB1. **e**, q-PCR shows the amount of rDNA in Col-0, *atx5 atx6*, *brca1 atx5 atx6*, *hop2 atx5 atx6*, and *cycb1 atx5 atx6*. Each dot in the bar plot represents one replicate, experiments were performed with 32 plants/replicate. Data are presented as mean \pm SD ($n = 3$ biological replicates). The relative amount of rDNA was normalized against *UBQ10*. (Unpaired two-tailed student t-test, *, **, *** and ****, $P < 0.05, 0.01, 0.001, \text{ and } 0.0001$, respectively). Source data are provided in the Source Data File.

Genotype	DNA re-replication	TEs re-activation	Activation of DDR	Virus resistance
Col-0	No	No	No	No
<i>atxr5 atxr6</i>	Yes	Yes	Yes	Yes
<i>brca1 atxr5 atxr6</i>	Yes	Yes	No	No
<i>mbd9 atxr5 atxr6</i>	No	No	No	No
<i>sac3b atxr5 atxr6</i>	No	No	No	No

Supplementary Table 1 Summary of the performance of triple mutants regarding the heterochromatin amplification, TE re-activation, DDR, and viral susceptibility.

Gene ID	Go enriched pathway	Go enriched pathway
AT2G01440	DNA repair	Response to DNA damage
AT2G17930	DNA repair	Response to DNA damage
AT3G50880	DNA repair	Response to DNA damage
AT1G15940	DNA repair	Response to DNA damage
AT1G20750	DNA repair	Response to DNA damage
AT2G31320	DNA repair	Response to DNA damage
AT2G31970	DNA repair	Response to DNA damage
AT3G07800	DNA repair	Response to DNA damage
AT3G02680	DNA repair	Response to DNA damage
AT3G27060	DNA repair	Response to DNA damage
AT3G24170	DNA repair	Response to DNA damage
AT4G21070	DNA repair	Response to DNA damage
AT4G25120	DNA repair	Response to DNA damage
AT4G25540	DNA repair	Response to DNA damage
AT5G02820	DNA repair	Response to DNA damage
AT5G45400	DNA repair	Response to DNA damage
AT5G61460	DNA repair	Response to DNA damage
AT3G27630		Response to DNA damage
AT1G68790		Response to DNA damage

Supplementary Table 2 GO analysis of 19 DDR genes from Fig. 2b

Sample_name	mt DNA Ratio
<i>atxr5 atxr6</i> Ino_rep1_Input	2.00%
<i>atxr5 atxr6</i> Ino_rep2_Input	2.09%
<i>atxr5 atxr6</i> Ino_rep1_RAD51	0.55%
<i>atxr5 atxr6</i> Ino_rep1_RPA1A	1.60%
<i>atxr5 atxr6</i> Ino_rep2_RAD51	0.56%
<i>atxr5 atxr6</i> Ino_rep2_RPA1A	1.53%
<i>atxr5 atxr6</i> Mock_rep1_Input	2.11%
<i>atxr5 atxr6</i> Mock_rep2_Input	2.03%
<i>atxr5 atxr6</i> Mock_rep1_RAD51	0.89%
<i>atxr5 atxr6</i> Mock_rep1_RPA1A	1.55%
<i>atxr5 atxr6</i> Mock_rep2_RAD51	0.77%
<i>atxr5 atxr6</i> Mock_rep2_RPA1A	1.52%
Col-0 Ino_rep1_Input	1.92%
Col-0 Ino_rep2_Input	1.95%
Col-0 Ino_rep1_RAD51	0.70%
Col-0 Ino_rep1_RPA1A	1.63%
Col-0 Ino_rep2_RAD51	0.80%
Col-0 Ino_rep2_RPA1A	1.48%
Col-0 Mock_rep1_Input	1.96%
Col-0 Mock_rep2_Input	1.96%
Col-0 Mock_rep1_RAD51	0.68%
Col-0 Mock_rep1_RPA1A	1.42%
Col-0 Mock_rep2_RAD51	0.74%
Col-0 Mock_rep2_RPA1A	1.46%

Supplementary Table 3 The ratios of mitochondria-mapped reads from CHIP-seq